Progress In Electromagnetics Research C, Vol. 87, 175–186, 2018

Theoretical Analysis for Systematic Design of Flexible Broadband Radar Absorbers Using the Least-Square Method

Thtreswar Beeharry[1, 2, *], Kamardine Selemani[2], Khadim Diakhoumpa[1], and Habiba H. Ouslimani[1]

Abstract—By taking into account the facts that thick dielectrics are required for low frequency absorbers, that thick dielectrics are not always flexible, and that targets are not always planar, an efficient tool for the systematic design of flexible broadband radar absorbers using the least-square method is presented in this paper. Two approaches for designing the physical model of the absorber are presented. The first one consists of resistive square loops deposited on top of a dielectric, and the second one consists of metallic square loops associated with lumped resistors. More than 90% of absorption rate is obtained in the required bandwidth for both transverse electric and transverse magnetic polarizations with the two approaches and achieving a performance of operational bandwidth to thickness ratio of 7.69. Finally, the required dimensions of flexible absorbers in some low frequency bands are given in order to show the versatility of the approach.

1. INTRODUCTION

One of the most common ways of reducing radar cross section for stealth technology is to use radar absorbers [1]. For practical reasons, broadband thin absorbers covering part or the whole frequency band of radars and antennas are best suitable for defense applications. Jaumann absorbers [2–4] and Salisbury screens [5–7] are very good examples of radar absorbers. Multilayer Jaumann absorbers suffer from large thickness as they are multiples of $\lambda/4$ (λ is the wavelength in free space) and bulkiness as each layer produces a single narrow band resonance. Based on metamaterials [8–11], Frequency Selective Surfaces (FSS) [3, 12, 13] are periodically arranged resonant structures printed on dielectric substrates. FSS often suffer from a narrow bandwidth (high quality factor because of their resonant structures). In order to enlarge the bandwidth, two popular techniques used, consists of incorporating resonating elements working at nearby frequencies by arranging them on the same plane [14, 15] or by using multi layers [16, 17] at the expense of a drop in the absorption at certain frequencies in the bandwidth and/or bulkiness. Genetic algorithms [18] and software based optimizations are also used to obtain broadband absorption. However with these methods the physical insight of how absorption is obtained is always debatable. Using well customized magnetic materials [18] can decrease the thickness but they can be very bulky and expensive. Well optimized honeycomb structures provide good absorption and are not bulky but are very fragile [19]. Moreover, target zones are not always planar, thus flexible or conformal radar absorbers are required. The thickness of dielectrics depending on the frequency range, non magnetic flexible dielectrics are not always available for low frequencies and the gigahertz regime. Moreover very few research has been done on non magnetic flexible broadband absorbers in the microwave regime [20]. For these reasons, designing flexible broadband radar absorbers for low frequencies of the microwave range with easily available dielectrics is very complicated and is a challenging topic. In this paper,

Received 22 August 2018, Accepted 2 October 2018, Scheduled 13 October 2018

* Corresponding author: Thtreswar Beeharry (tbeeharry@cmn-cherbourg.com).

[1] Laboratoire Energétique Mécanique Electromagnétisme, Université Paris Nanterre, Ville d'Avray 92410, France. [2] Constructions Mécaniques de Normandie, Systems Department, Cherbourg 50105, France.

an efficient way of designing flexible non-magnetic broadband radar absorbers using the least-square method and the equivalent Transmission Line Model (TLM) is described. The C band is taken as an example to illustrate the proposed method.

2. TRANSMISSION LINE MODEL FOR PERFECT ABSORPTION

One straight forward solution to design a radar absorber is to place a complex sheet (surface providing complex impedance) over a grounded dielectric as shown in Figure 1. The complex sheet is designed in a way that the whole structure matches the impedance of the free space ($Z_0 = 377\,\Omega$). Let us assume that we want to design a flexible broadband non magnetic absorber in the frequency range of 3.5–7 GHz which achieves at least -10 dB of reflection (at least 90% of absorption) in the given range. Three parameters are important for the design of the absorber: the thickness and permittivity of the dielectric substrate and the geometrical parameters of the complex sheet.

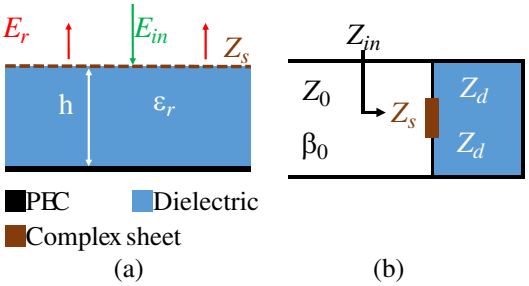

Figure 1. (a) Schematic design of a radar absorber. (b) Transmission line model of the absorber.

Using the transmission line theory, the impedance of the grounded substrate for normal incidence is given by [21]:

$$Z_g = jZ_d \tan(\beta_d h), \tag{1}$$

where $Z_d = \sqrt{\mu_0/\epsilon_0\epsilon_r}$ is the characteristic impedance of the dielectric, and $\beta_d = \frac{\omega\sqrt{\epsilon_r}}{c}$ is the propagation constant in the dielectric. The input impedance, Z_{in}, is given by the parallel combination of the grounded dielectric (Z_g) and the complex sheet (Z_s):

$$Z_{in} = \frac{jZ_s Z_d \tan(\beta_d h)}{Z_s + jZ_d \tan(\beta_d h)} \tag{2}$$

For perfect absorption, the reflexion must satisfy $R = (Z_{in} - Z_0)/(Z_{in} + Z_0) = 0$. Hence, perfect absorption is obtained when $Z_{in} = Z_0$. The required impedance of the complex sheet, Z_{Req}, for perfect absorption, satisfying $Z_{in} = Z_0$ is given by:

$$Z_{Req} = \frac{Z_0 Z_d \tan(\beta_d h)}{jZ_0 + Z_d \tan(\beta_d h)} \tag{3}$$

From Equation (3), it can be seen that the required complex sheet for perfect absorption depends on the permittivity and the thickness of the dielectric. The required complex impedance for different thicknesses is plotted according to Equation (3) in Figure 2. The permittivity of the substrate is fixed at $\epsilon_r = 3$ (lossless rubber). The substrate is chosen to be rubber because it is flexible and can be conformed to any target even if it is thick.

For example, at 4 GHz and 6 mm thick dielectric (blue curves of Figure 2), the required complex sheet impedance for perfect absorption is $Z_{Req} = 120.1 - j175.59\,\Omega$. It should be noted that positive values of the imaginary part of Z_{Req} imply that an inductive response is needed and negative values require capacitive response. Hence in this example, the complex sheet must be capacitive whose TLM can be given by a series of Resistor-Capacitor circuit in parallel of the 6 mm thick grounded transmission line. The value of the required resistor is directly given by $\mathrm{Re}(Z_{Req})$ which is $120\,\Omega$ in our case. The

value of the of the capacitor is given by equating the impedance of the capacitor $(1/jC\omega)$ to $-j175.59$. C is found to be equal to 0.227 pF. For a grounded absorber, the absorption is given by:

$$A = 1 - |R|^2, \tag{4}$$

where R is the reflexion coefficient (S_{11} parameter). The reflexion is given by $R = (Z_{in} - Z_0)/(Z_{in} + Z_0)$. Figure 3 shows a perfect absorption rate of the designed absorber at 4 GHz.

The simulation was done using commercial CST Design Studio Suite 2017. Periodic boundary conditions were applied in the numerical model in order to mimic a 2D infinite structure. Floquet ports were used for the excitation and the period of the structure was equal to $\lambda/20$. An excellent agreement was found between the analytical model and simulated CST results.

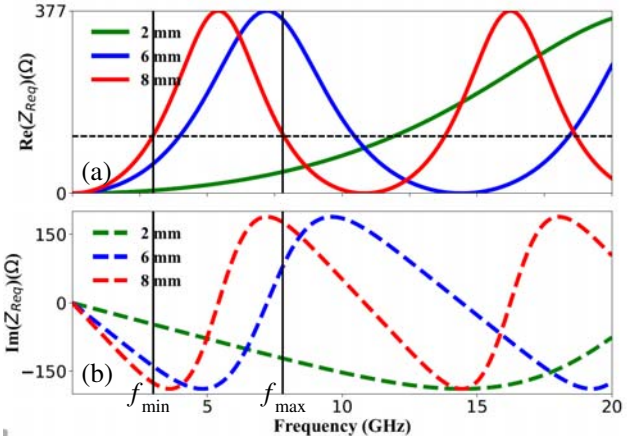

Figure 2. (a) Real part of required impedance. (b) Imaginary part of required impedance. The two solid vertical black lines represent the $f_{\min} = 3$ GHz and $f_{\max} = 7.8$ GHz limits which is our frequency band design goal used in Section 3.

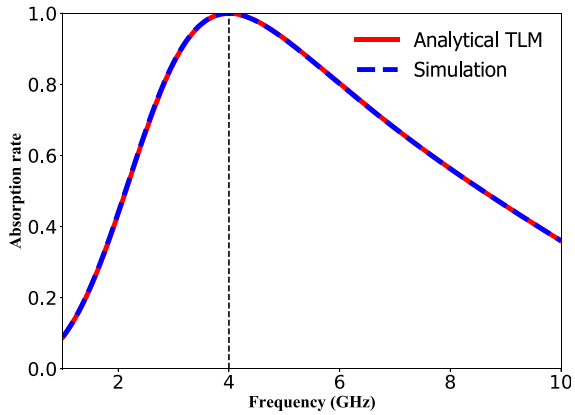

Figure 3. Analytical and simulated absorption rates.

3. DESIGN STRATEGY FOR BROADBAND ABSORPTION

3.1. Determination of Dielectric Thickness

The strategy we adopt in this work is to achieve perfect absorption at $f_{\min}$ and $f_{\max}$ where $f_{\min}$ and $f_{\max}$ are the lower and upper limits of the desired frequency band respectively. To do so, the thickness must be selected such that the imaginary part of the required impedance, $\mathrm{Im}(Z_{Req})$, have the same values at $f_{\min}$ and $f_{\max}$ but must be exactly out of phase. In this case we must observe $\mathrm{Im}(Z_{Req})$ increasing from being negative to positive and $\mathrm{Re}(Z_{Req})$ must have the same values at $f_{\min}$ and $f_{\max}$. In our design goal, $f_{\min} = 3$ GHz and $f_{\max} = 7.8$ GHz, the 8 mm ($\lambda/7$ thin at the center frequency of 5.4 GHz) dielectric thickness satisfies the conditions described above (see Figure 2). It can be observed with the red curves that $\mathrm{Im}(Z_{Req}) = -170\,\Omega$ at $f_{\min}$ and $\mathrm{Im}(Z_{Req}) = +170\,\Omega$ at $f_{\max}$. Also, $\mathrm{Re}(Z_{Req}) = 118\,\Omega$ at both $f_{\min}$ and $f_{\max}$.

3.2. Determination of Complex Sheet Parameters

As observed in Figure 2, $\mathrm{Im}(Z_{Req})$ is both positive and negative between 3 and 7.8 GHz. The complex sheet must be both capacitive and inductive and must be the closest possible to $\mathrm{Im}(Z_{Req})$. The TLM is hence given by a series of Resistance-Capacitor-Inductor (RLC) circuit in parallel of the 8 mm thick grounded transmission line as shown in Figure 4.

In the TLM of Figure 4, the resistance, R_s, will take into account the resistive losses ($\mathrm{Re}(Z_{Req})$). The absorption optimization based on the losses will be discussed later. The impedance of a series RLC

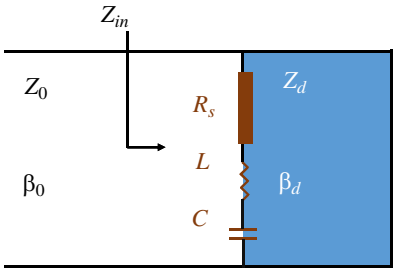

Figure 4. TLM model proposed for broadband absorption.

circuit is given by:

$$Z_{RLC} = R_s + j\frac{LC\omega^2 - 1}{C\omega}, \tag{5}$$

where ω is the angular frequency. As stated previously we want to have perfect absorption at $f_{\min}$ and $f_{\max}$ in a first time. The imaginary part of Equation (5) must be equal to $\mathrm{Im}(Z_{Req})$ at $f_{\min}$ and $f_{\max}$ leading to the following condition:

$$-C \cdot \mathrm{Im}(Z_{Req}) \cdot \omega + L \cdot C \cdot \omega^2 = 1 \tag{6}$$

For simplicity we let $\mathrm{Im}(Z_{Req}) = z_r$. As z_r is frequency dependent, Equation (6) can be written in the following matrix form:

$$\begin{bmatrix}1\\1\end{bmatrix} = \begin{bmatrix}-z_r(\omega_{\min}) \cdot \omega_{\min} & \omega_{\min}^2\\ -z_r(\omega_{\max}) \cdot \omega_{\max} & \omega_{\max}^2\end{bmatrix}\begin{bmatrix}C\\LC\end{bmatrix} = \psi\begin{bmatrix}C\\LC\end{bmatrix} \tag{7}$$

where ψ is a $(2 * 2)$ matrix. C and LC can be calculated using the least square method [22] such that is fits z_r. Let us take a simple example to see how we can use the least square method in our case: Let us consider the following linear equation: $y = dx + c$. We also know that the line passes around three different position: (x_1, y_1), (x_2, y_2) and (x_3, y_3). In this case, we should have, $c + dx_1 = y_1$, $c + dx_2 = y_2$ and $c + dx_3 = y_3$. If there are no errors about these three points, then the three equations would be correct and c and d would be determined by only two of the equations. However in the presence of errors the system is inconsistent. The idea of the least square method is that it minimizes the sum of the errors namely $(c + dx_1 - y_1)^2$, $(c + dx_2 - y_2)^2$ and $(c + dx_3 - y_3)^2$. In general, for an overdetermined $m * n$ system $Ax = b$, what Gauss and Legendre discovered is that there are solutions x minimizing $||Ax - b||^2$ and that these solutions are given by the square $n * n$ system $A^TAx = A^Tb$. When the columns of A are linearly independent, it turns out that A^TA is invertible, and so x is unique and given by $x = (A^TA)^{-1}A^Tb$. A^TA is a symmetric matrix, one of the nice features of the so-called normal equations of a least squares problem. Thus in our case we can write:

$$\begin{bmatrix}C\\LC\end{bmatrix} = (\psi^T\psi)^{-1}\psi^T\begin{bmatrix}1\\1\end{bmatrix}, \tag{8}$$

where ψ^T is transpose of the matrix ψ. From Equation (8), the value of the capacitance is given by C directly and the value of L is given by LC/C. In our case, $L = 5.84\,\mathrm{nH}$ and $C = 0.186\,\mathrm{pF}$ are obtained. Figure 5 shows the imaginary part of the LC series impedance. It can be observed that the imaginary part of the complex sheet's impedance whose values of L and C has been calculated using Equation (8), is exactly the same as the required imaginary part of impedance at $f_{\min}$ and $f_{\max}$ validating Equation (8).

At this stage, all the TLM parameters of the absorber for a broadband absorption between 3 and 7.8 GHz are known. The thickness of the dielectric $h = 8\,\mathrm{mm}$ having $\epsilon_r = 3$. The initial resistance of the complex sheet $R_s = 118\,\Omega$ and L and C values are of $L = 5.84\,\mathrm{nH}$ and $C = 0.186\,\mathrm{pF}$, respectively. By substituting Z_{RLC} of Equation (5) to Z_s in Equation (2) and using Equation (4), the absorption rate of the TLM of the absorber is plotted in Figure 6 for different values of R_s.

It can be seen that with the initial value R_s, which is $118\,\Omega$ (black curve), perfect absorption is obtained at 3 GHz and 7.8 GHz respectively (as expected), but the absorption is less than 90% in the

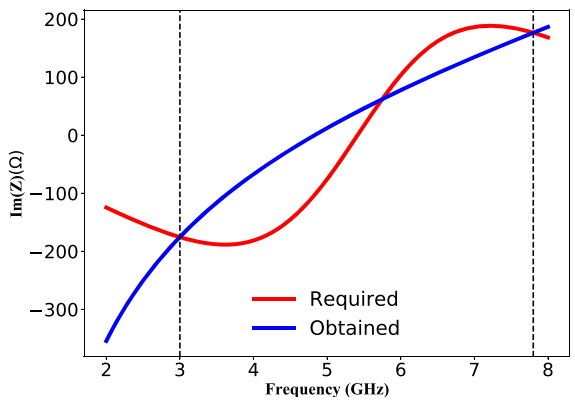

Figure 5. Comparison between Im(Z) required and calculated Im(Z) using Equation (8) of the LC model.

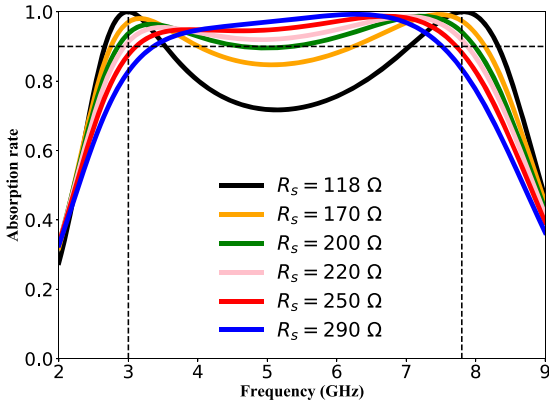

Figure 6. Absorption rate for different values of resistance.

3–7.8 GHz band. This result is logical as the RLC model has been matched at 3 GHz and 7.8 GHz respectively and not in the whole band. It can also be observed that when the complex sheet is made more lossy, by increasing the value of its real part (R_s), the absorption is enhanced and for values of R_s greater than 200 Ω, the absorption is at least of 90% in the whole band of 3–7.8 GHz. R_s cannot be increased infinitely since the bandwidth becomes very narrow, as it can be observed for $R_s = 290\,\Omega$ in Figure 6. Thus R_s must be carefully selected. For our case, $R_s = 200\,\Omega$ is selected as the absorption is at least of the 90% in the whole band of 3–7.8 GHz. To recapitulate, the final TLM parameters of the complex sheet impedance are: $R_s = 200\,\Omega$, $L = 5.84$ nH and $C = 0.186$ pF.

3.3. Physical Model

Extensive research has been done on equivalent circuit models of FSS taking into consideration its geometry [22–25]. In this work, simple square loop arrays will be used to design the complex sheet in order to obtain an inductive and a capacitive response of $L = 5.84$ nH and $C = 0.186$ pF respectively. A well dimensioned infinite array of square loops can give a capacitive and inductive response and hence Im(Z_{Req}). The arrays of square loops have been designed as described in [25]. In order to get the required resistive response that is Re(Z_{Req}), the square loops can be made of Ohmic sheets or of PEC including lumped resistances.

3.3.1. Square Arrays Made of Resistive Films

The relations between L and C values and the dimensions of the square loops can be found in [25]. Figure 7 depicts the top view of the a unit cell of square loops placed on top of the 8 mm thick grounded dielectric.

The unit cell has a period p of 10 mm, and the square array has a length d of 9.5 mm and width s equal to 0.15 mm. The relationship between the value of the required real part, $R_s = 200\,\Omega$, and the value of the resistive sheet is related by Equation (9) as described in [25].

$$R_s = R_{OhmicSheet}\frac{S}{A}, \tag{9}$$

where S is the surface area of the unit cell, and A represents the elements along which currents propagate on the square loop. In our case, for Transverse Electric (TE) polarization, A is the surface area of the two vertical arms of the square loop, $S = 0.1\,\text{mm}^2$, $A = 2.85\,\mu\text{m}^2$, $R_s = 200\,\Omega$ and thus the resistance of our ohmic sheet, $R_{OhmicSheet} = 5.7\,\Omega$/Square. Commercial CST Design Studio Suite using the same conditions as in Section 2 has been used to perform the simulation of the structure. Figure 8 depicts the simulated absorption rate of the structure for linearly co-polarized TE and TM waves under oblique incidences.

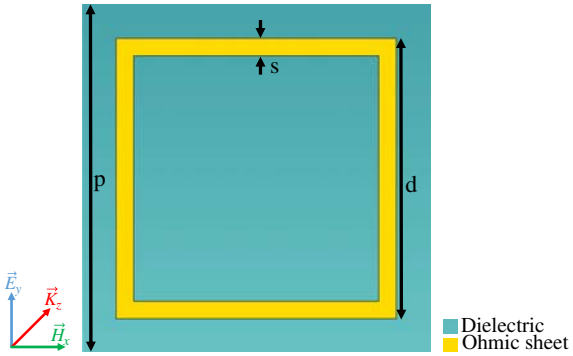

Figure 7. Top view of the unit cell of squared ohmic sheet placed on a 8 mm grounded dielectric.

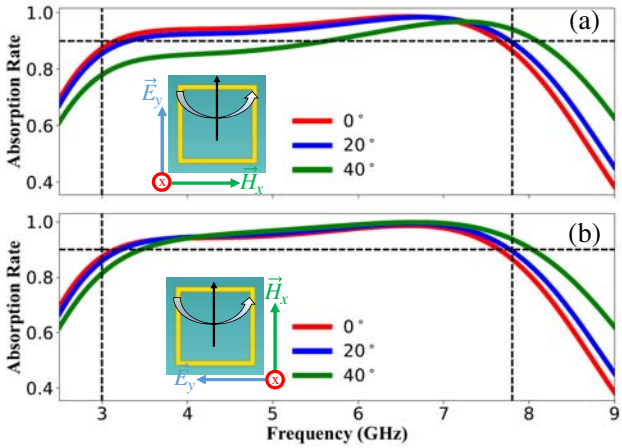

Figure 8. Absorption rate of the proposed structure under oblique incidences of 0–40°. (a) TE polarization. (b) TM polarization.

From Figure 8, it can be observed that for both TE and TM polarizations, that for normal incidence and oblique incidences of until 20° (red and blue curves) the absorption rate is more than 90/% (less than −10 dB of reflection) in the whole band of 3–7.8 GHz which was our design goal. Results for incidence angles of until 40° (green curve) shows that the absorption band decreases but remain interesting. The absorption rates for TE and TM polarizations are the same for normal incidence as the square arrays are completely symmetrical along x and y axes. These results validates the proposed design strategy as more than 90% of absorption is obtained in the whole band of 3–7.8 GHz.

3.3.2. Square Arrays Made of PEC with Lumped Resistors

Metallic (or PEC) square arrays associated with lumped resistors can also be used in order to have the required impedance, Z_{Req}. The dimensions of the square arrays, which gives the required imaginary part for broadband absorption, $\mathrm{Im}(Z_{Req})$, remains the same as for the resistive square arrays in Section 3.3.1. Since PEC is not lossy, additional resistors (optimized value and number) must be added in the square arrays so that broadband absorption is obtained. Figure 10, represents the top view of the absorber. Furthermore, as we want to design a flexible absorber and want to use rubber as dielectric, one can not print the PEC square arrays on rubber. The proposed solution is to place 0.1 mm thick FR4 substrate ($\epsilon_r = 4.2 - j0.105$) placed on top of a 7.9 mm grounded rubber ($\epsilon_r = 3$) substrate. The metallic square arrays are printed on the 0.1 mm thick FR4 substrate. In our case, the 0.1 mm thick FR4 being very small compared to the 7.9 mm thick rubber and their permittivity being close to each other, the overall effective permittivity is around $\epsilon_r = 3$. In Figure 9 the real part and imaginary part of the effective permittivity of a 0.1 mm thick FR4 substrate placed on top of a 7.9 mm thick rubber substrate has been retrieved and calculated as described in [26]. The effective permittivity can be observed to be around $\epsilon_{eff} = 3 - j0$.

The structure of the absorber is now a 0.1 mm thick FR4 substrate on which the square arrays are printed, placed on top of a 7.9 mm thick grounded rubber.

The square arrays have the same dimensions p, d and s as in Section 3.3.1. Optimized gaps of dimension, $g = 1$ mm have been added in order to connect the resistors R_E and R_H. The resistors, R_E and R_H are set at 220 Ω. From Figure 6, it can be seen that for values of R_s between 200 and 250 Ω, the absorption remains more than 90% in the 3–7.8 GHz range. Hence the surface impedance of the square loop including the lumped resistors can be between 200 and 250 Ω. The number of resistors in each arm of the square loops will give different surface impedances and absorption. In the figure below, the absorption rate for different numbers of 220 Ω resistors is plotted. It must be noted that any value of resistor, R_s, can be chosen, but the surface impedance of the square loop including the lumped resistors must be between 200 and 250 Ω.

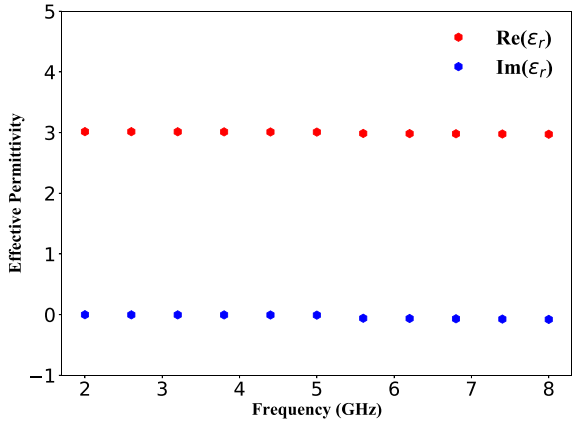

Figure 9. Retrieved real part (red curve) and imaginary part (blue curve) of the effective permittivity of a 0.1 mm thick FR4 substrate placed on top of a 7.9 mm thick rubber substrate.

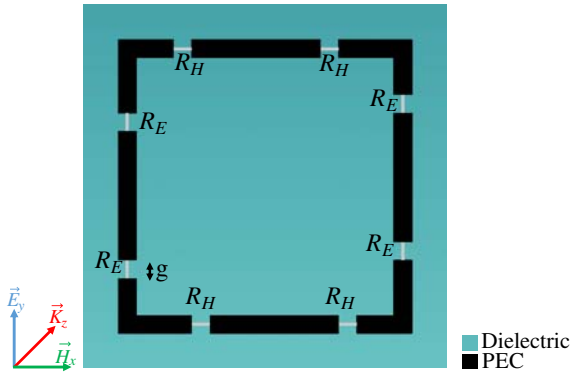

Figure 10. Top view of the unit cell of a PEC square array printed on FR4 substrate placed on top of a 7.9 mm grounded rubber dielectric.

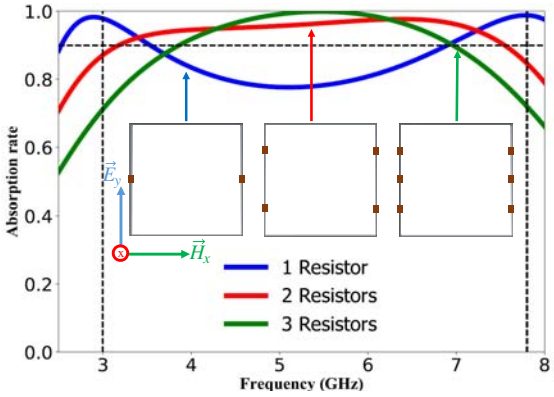

Figure 11. Absorption rate of the PEC with one, two and 3 resistors in the two vertical arms. The structures were simulated for linearly polarized TE wave.

Figure 11 shows the absorption rate of the square arrays with varying numbers of resistors in the vertical arms for the TE polarization case. It can be observed that for 1 resistor (blue curve) of 220 Ω in the two vertical arms, the absorption rate is more than 90% at 3 GHz and 7.8 GHz respectively but do not provide a surface impedance between 200 and 250 Ω. Following the same reasoning, two resistors (red curve) do provide the necessary surface impedance as the absorption rate is more than 90% in the whole band of 3–7.8 GHz (very slightly less in bandwidth but the resistors can be tuned and get a bandwidth of exactly 3–7.8 GHz). In the case when 3 resistors (green curve) are added, the surface impedance is very big compared to what is required and perfect absorption is obtained between 5 and 6 GHz, but the bandwidth is reduced as we could have deduced from Figure 6. Thus two 220 Ω resistors in the two vertical arms are maintained in the designed of our broadband absorber for TE polarization. Our structure being perfectly symmetrical 220 Ω resistors are maintained on the horizontal arms of the square arrays for TM polarization. For TE polarization, maximum currents flow on the vertical arms of the square arrays, and maximum currents flow in the horizontal arms for TM polarization as shown in Figure 12.

The resistors R_E bring the required losses for TE polarization and resistors R_H bring losses for TM polarization. Depending on which polarization we are working on, R_E or R_H can be removed from the arms on which currents are not flowing, must be made with continuous PEC (with no gaps, g). In some applications where both TE and TM are required, the gaps, g, must be optimized such

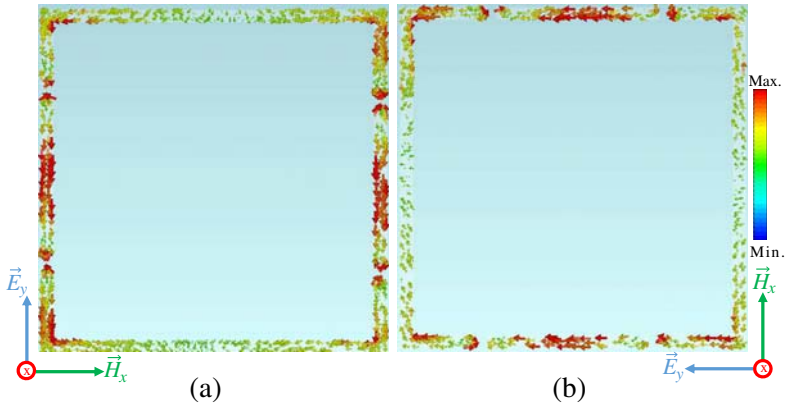

Figure 12. (a) Maximum currents flow on the vertical arms for TE polarization at 5.5 GHz. (b) Maximum currents flow on the horizontal arms for TM polarization at 5.5 GHz.

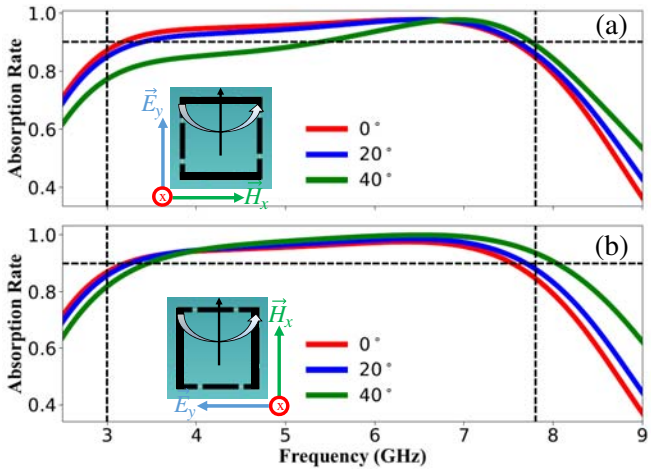

Figure 13. Absorption rate of the proposed structure under oblique incidences of 0–40°. (a) TE polarization. (b) TM polarization.

that the imaginary part of the required impedance does not change significantly (as the gaps will bring some capacitive effects). Figure 13 depicts the simulated absorption rate of the structure for linearly polarized TE (a) and TM (b) waves under oblique incidences.

It can be seen from Figure 8, for both TE and TM polarizations, that for normal and oblique incidences of until 20° (red, blue curves) the absorption rate is more than 90% in the whole band of 3.09–7.7 GHz. These results are slightly less than 3–7.8 GHz band but the two resistors of each arms can be tuned around 220 Ω in order to have the exact bandwidth. The same trends are observed for higher incidences as in Section 3.3.1. These results also validate the proposed design strategy for broadband absorption.

4. EXAMPLES AND PERFORMANCE

In order to show the versatility of the proposed design plan, the methods used in Section 3 have been applied to some low frequency bands. Table 1 shows the TLM elements required for at least 90% of absorption in these desired frequency bands. In each case rubber ($\epsilon_r = 3$) was selected as dielectric whose thickness is given in column 2 of Table 1. We have purposely selected some low frequency bands for which the dielectric thickness is not negligible and classical dielectrics are not flexible for large thicknesses. For the cases studied in the table below, slabs of 10 mm thick flexible rubber can be put

Table 1. TLM model elements for flexible absorbers in some low frequency bands.

Example	Desired Band (GHz)	Thickness (mm)	R_s (Ω)	L (nH)	C (pF)
1	0.3–0.6	90	250	77.18	1.69
2	0.5–0.9	60	250	52.6	1.09
3	1–2.4	25	250	19.85	0.52

Table 2. Dimensions of physical model of radar absorbers using square loop arrays made of resistive sheets for the same bands as in Table 1.

Example	Desired Band (GHz)	$R_{OhmicSheet}$ (Ω/square)	p (mm)	d (mm)	s (mm)
1	0.3–0.6	0.86	80	75	0.147
2	0.5–0.9	1.2	60	55	0.160
3	1–2.4	1.43	25	24	0.127

on top of each other making the whole system flexible.

In order to design the square loop arrays with PEC using lumped resistors, the dimensions of p, d and s remain the same as in Table 2. Two lumped resistors of 220 Ω must be added to each arm as described in Section 3.3.2. The PEC square loops must be printed on a 0.1 mm FR4 substrate (or any other substrate but the overall effective permittivity must be around 3) as explained in Section 3.3.2.

The performance of an absorber is often judged upon its 90% absorption rate band to center frequency ratio given by $(f_{\max} - f_{\min})/f_c$, where f_c is the center frequency. This criteria does not take into consideration the thickness of the absorber which can be the most important factor in some applications. The operational bandwidth to thickness ratio to evaluate the performance of the absorber is used this work. Operational bandwidth to thickness ratio is given by $(\lambda_{f\min} - \lambda_{f\max})/h$, where $\lambda_{f\min}$ and $\lambda_{f\max}$ are the wavelengths at $f_{\min}$ and $f_{\max}$ respectively, and h is the thickness of the absorber. The bigger is this ratio, the better operational bandwidth to thickness ratio performance an absorber has. Table 3 is a comparison of designed absorbers in this paper with some other absorbers.

When fixing the permittivity of the dielectric substrate of an absorber, as in this work, the 90% absorption rate band to center frequency ratio (column 4 of Table 3) or operational bandwidth to

Table 3. Performance comparison of our absorber with some other absorbers.

Reference	90% absorption band (GHz)	thickness (mm)	$(f_{\max} - f_{\min})/f_c$ (%)	$(\lambda_{f\min} - \lambda_{f\max})/h$	Flexible
[27]	7–18	4.36	88	6	No
[20]	5.8–12.2	5	71.1	5.42	Yes
[28]	8.37–21	3.65	86	5.9	No
This work (Example 1)	0.3–0.6	90	66.6	5.55	Yes
This work (Example 2)	0.5–0.9	60	57	4.44	Yes
This work (Example 3)	1–2.4	25	82.3	7	Yes
This work (Design Goal)	3–7.8	8	88.8	7.69	Yes

thickness ratio (column 5 of Table 3) performances can be affected as the degrees of freedom for optimization is reduced. With the design approach proposed in this method, it can be clearly seen from Table 3 that, very high performances can be achieved with the proposed method even by fixing the permittivity of the dielectric substrate. In fact 88% for the 90% absorption rate band to center frequency ratio and an operational bandwidth to thickness ratio of 7.69 are obtained making the proposed design strategy very competitive.

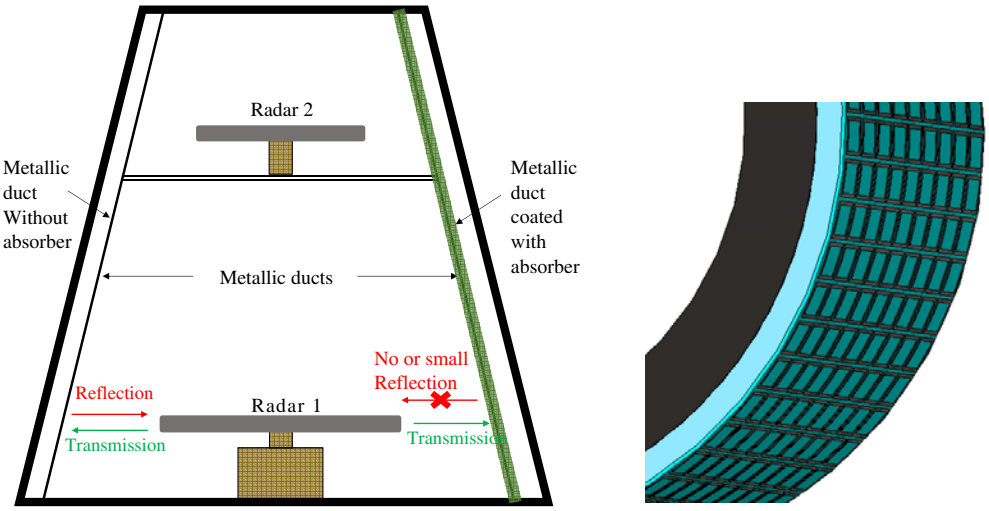

Figure 14. (a) Representation of a metallic duct inside a radome. On the left, the metallic duct is not covered and on the right the mettalic duct is covered by a flexible radar absorber. (b) Illustration of the presented absorber conformed on a non planar metallic duct.

5. CONCLUSION

In this paper, a simple but powerful analytical tool to design broadband flexible radar absorbers for any frequency band using the TLM is presented. Firstly, the expressions to calculate the required real and imaginary parts of impedances for broadband absorptions for any dielectric permittivity and thickness are given. The real part of the required impedance has been associated to a resistance and the imaginary part has been associated to an inductor and a capacitor in series. A simple matrix formulation is used to get the values of L and C that fits the required imaginary part of the impedance at the lower and upper limits of the frequency band. We have shown that broadband absorption can be achieved by increasing the value of the resistance in the TLM. Finally, once all the parameters of the TLM model found, two physical model approaches using square arrays to design the absorber are described. The first approach consists of using resistive sheets patterned as square arrays. The dimensions of the arrays and the unit cell will give the required imaginary part of impedance. The required real part of impedance is given by the resistance value of the resistive films. The second approach is to use printed metallic square arrays on a dielectric substrate. As for the first approach, the dimensions of the arrays and the unit cell will give the required imaginary part of impedance. The real part of the impedance is obtained by including lumped resistors in the arms of the square arrays. In both cases the square arrays being symmetrical, broadband absorptions for both linearly polarized TE and TM modes are obtained. Also the proposed absorbers achieve as 88% for the 90% absorption rate band to center frequency ratio and an operational bandwidth to thickness ratio of 7.69 making the proposed design strategy extremely interesting. Communication devices such as detection radars working on the X band frequency range, one suitable application of the absorber is to reduce back scattering from metallic objects in radomes of military vessels. For example, several antennas and radars are mounted inside radomes which may contain metallic objects such as cable ducts. Reflected electromagnetic waves due to these metallic

objects cause EMI critical issues such as saturation of source antennas and radars. The metallic ducts also cause indirect echoes, shadow and blind zones. Covering metallic parts with radar absorbers can decrease considerably the reflections, and hence the indirect echoes. This is illustrated in Figure 14.

It should be noted that further studies must be done in order to conform the absorber to cyclindrical metallic objects as the reflexion will depend of the radius of the mettalic targets. As we have done all studies for planar radar absorbers, if we had to conform it to a mettalic cylinder, the radius of the cylinder must be much bigger than the wavelength. The RCS results of the absorber conformed around metallic objects are not presented in this article as further optimization studies must be carried.

ACKNOWLEDGMENT

This work was developed in collaboration with the SYSTEMS department of Constructions Mécaniques de Normandie (CMN).

REFERENCES

1. Emerson, W., "Electromagnetic wave absorbers and anechoic chambers through the years," *IEEE Transactions on Antennas Propag.*, Vol. 21, 484–490, 1973.
2. Chambers, B. and A. Tennant, "Design of wideband Jaumann radar absorbers with optimum oblique incidence performance," *Electron. Lett.*, Vol. 30, 1530–1532, 1994.
3. Munk, B. A., P. Munk, and J. Pryor, "On designing Jaumann and circuit analog absorbers (ca absorbers) for oblique angle of incidence," *IEEE Transactions on Antennas Propag.*, Vol. 55, 186–193, 2007.
4. Chambers, B. and A. Tennant, "Optimised design of Jaumann radar absorbing materials using a genetic algorithm," *IEE Proceedings — Radar, Sonar Navig.*, Vol. 143, 23–30, 1996.
5. Chambers, B., "Optimum design of a salisbury screen radar absorber," *Electron. Lett.*, Vol. 30, 1353–1354, 1994.
6. Fante, R. L. and M. T. Mccormack, "Reflection properties of the salisbury screen," *IEEE Transactions on Antennas Propag.*, Vol. 36, 1443–1454, 1988.
7. Chambers, B., "Frequency tuning characteristics of capacitively loaded salisbury screen radar absorber," *Electron. Lett.*, Vol. 30, 1626–1628, 1994.
8. Veselago, V. G., "The electrodynamics of substances with simultaneously negative values of ε and μ," *Sov. Physics Uspekhi*, Vol. 10, 509, 1968.
9. Alitalo, P. and S. Tretyakov, "Electromagnetic cloaking with metamaterials," *Mater. Today*, Vol. 12, 22–29, 2009.
10. Landy, N. I., S. Sajuyigbe, J. Mock, D. Smith, and W. Padilla, "Perfect metamaterial absorber," *Phys. Review Letters*, Vol. 100, 207402, 2008.
11. Smith, D. R., W. J. Padilla, D. Vier, S. C. Nemat-Nasser, and S. Schultz, "Composite medium with simultaneously negative permeability and permittivity," *Phys. Review Letters*, Vol. 84, 4184, 2000.
12. Tennant, A. and B. Chambers, "A single-layer tuneable microwave absorber using an active fss," *IEEE Microw. Wirel. Components Lett.*, Vol. 14, 46–47, 2004.
13. Zadeh, A. K. and A. Karlsson, "Capacitive circuit method for fast and efficient design of wideband radar absorbers," *IEEE Transactions on Antennas Propag.* Vol. 57, 2307–2314, 2009.
14. Jing, L., Z. Wang, Y. Yang, B. Zheng, Y. Liu, and H. Chen, "Chiral metamirrors for broadband spin-selective absorption," *Appl. Phys. Lett.*, Vol. 110, 231103, 2017.
15. Sood, D. and C. C. Tripathi, "Broadband ultrathin low-profile metamaterial microwave absorber," *Appl. Phys. A*, Vol. 122, 332, 2016.
16. Beeharry, T., R. Yahiaoui, K. Selemani, and H. H. Ouslimani, "A dual layer broadband radar absorber to minimize electromagnetic interference in radomes," *Sci. Reports*, Vol. 8, 382, 2018.

17. Ghosh, S., S. Bhattacharyya, and K. V. Srivastava, "Design, characterisation and fabrication of a broadband polarisation-insensitive multi-layer circuit analogue absorber," *IET Microwaves, Antennas and Propag.*, Vol. 10, 850–855, 2016.
18. Chen, H., Z. Wang, R. Zhang, H. Wang, S. Lin, F. Yu, and H. O. Moser, "A meta-substrate to enhance the bandwidth of metamaterials," *Sci. Reports*, Vol. 4, 5264, 2014.
19. Feng, J., Y. Zhang, P. Wang, and H. Fan, "Oblique incidence performance of radar absorbing honeycombs," *Compos. Part B: Eng.*, Vol. 99, 465–471, 2016.
20. Jang, T., H. Youn, Y. J. Shin, and L. J. Guo, "Transparent and flexible polarization-independent microwave broadband absorber," *Acs Photonics*, Vol. 1, 279–284, 2014.
21. Tretyakov, S., *Analytical Modeling in Applied Electromagnetics*, Artech House, 2003.
22. Lee, D., N. T. Trung, U.-C. Moon, and S. Lim, "Optimal parameter retrieval for metamaterial absorbers using the least-square method for wide incidence angle insensitivity," *Appl. Optics*, Vol. 56, 4670–4674, 2017.
23. Singh, D., A. Kumar, S. Meena, and V. Agarwala, "Analysis of frequency selective surfaces for radar absorbing materials," *Progress In Electromagnetics Research B*, Vol. 38, 297–314, 2012.
24. Costa, F., S. Genovesi, A. Monorchio, and G. Manara, "A circuit-based model for the interpretation of perfect metamaterial absorbers," *IEEE Transactions on Antennas Propag.*, Vol. 61, 1201–1209, 2013.
25. Langley, R. J. and E. A. Parker, "Equivalent circuit model for arrays of square loops," *Electron. Lett.*, Vol. 18, 294–296, 1982.
26. Chen, X., T. M. Grzegorczyk, B.-I. Wu, J. Pacheco, Jr., and J. A. Kong, "Robust method to retrieve the constitutive effective parameters of metamaterials," *Phys. Rev. E*, Vol. 70, 016608, 2004.
27. Long, C., S. Yin, W. Wang, W. Li, J. Zhu, and J. Guan, "Broadening the absorption bandwidth of metamaterial absorbers by transverse magnetic harmonics of 210 mode," *Sci. Reports*, Vol. 6, 21431, 2016.
28. Xiong, H., J.-S. Hong, C.-M. Luo, and L.-L. Zhong, "An ultrathin and broadband metamaterial absorber using multi-layer structures," *J. Appl. Phys.*, Vol. 114, 064109, 2013.